Nanoscale

PAPER

Magnetic study on biodistribution and biodegradation of oral magnetic nanostructures in the rat gastrointestinal tract

Cite this: DOI: 10.1039/c6nr04678a

Miguel Martín,[a] Alba Rodríguez-Nogales,[b] Víctor Garcés,[a] Natividad Gálvez,[a] Lucía Gutiérrez,*[c] Julio Gálvez,[b] Deyanira Rondón,[d] Mónica Olivares[d] and Jose M. Dominguez-Vera*[a]

Received 9th June 2016,
Accepted 16th July 2016

DOI: 10.1039/c6nr04678a

www.rsc.org/nanoscale

We have undertaken a magnetic study on the oral biodistribution and biodegradation of nude maghemite nanoparticles of 10 nm average size (MNP) and probiotic bacteria, *Lactobacillus fermentum*, containing thousands of these same nanoparticles (MNP–bacteria). Using AC magnetic susceptibility measurements of the stomach, small intestine, cecum and large intestine obtained after rat sacrifice, and iron content determination by ICP-OES, we have monitored the biodistribution and biodegradation of the maghemite nanoparticles along the gastrointestinal tract, after oral administration of both MNP and MNP–bacteria. The results revealed that the amount of magnetic nanoparticles accumulated in intestines is sensibly higher when MNP–bacteria were administered, in comparison with MNP. This confirms our initial hypothesis that the use of probiotic bacteria is a suitable strategy to assist the magnetic nanoparticles to overcome the stomach medium, and to achieve their accumulation in intestines. This finding opens doors to different applications. Since iron absorption in humans takes place precisely in the intestines, the use of MNP–bacteria as an iron supplement is a definite possibility. We have actually illustrated how the administration of MNP–bacteria to iron-deficient rats corrects the iron levels after two weeks of treatment.

Introduction

The unique magnetic properties of magnetite (Fe_3O_4)/maghemite (γ-Fe_2O_3) iron oxide nanoparticles, their biodegradability and low toxicity have paved the way for various biomedical applications, including Magnetic Resonance Imaging (MRI), drug delivery and magnetically induced therapeutic hyperthermia.[1–10] However, the efficiency of iron oxide nanoparticles as drugs requires the control of two crucial processes: biodistribution and biodegradation. After their administration, the iron oxide nanoparticles have, first, to specifically accumulate into the tissue to be imaged or treated, and secondly to be degraded in an adequate manner and time to reduce potential toxic effects.[11]

Most magnetite/maghemite nanoparticles reported for biomedical applications need to be administered by injection. However, when the target is located at the gastrointestinal tract (GI), oral drug administration is usually a more convenient route, because it avoids the discomfort and additional procedures associated with intravenous delivery injections. Oral delivery through organs in the gastrointestinal tract (GI) needs to overcome a couple of important obstacles: the strong acidic gastric environment that reduces drug stability, and the digestive enzymes that degrade drugs, thus decreasing their bioavailability. Data on biodistribution and biodegradation of magnetic nanoparticles through the GI are currently still scarce[12] despite the opportunities that nanoparticles offer nowadays in diagnosis and therapy of diseases in such an area, such as intestines. Here is where the major diseases develop, such as inflammatory bowel disease or colorectal cancer, the third most common type of cancer, with 700 000 deaths in 2012.[13]

Furthermore, magnetite/maghemite nanoparticles have emerged as new physical and chemical forms to control iron deficiency. Iron has been recognized to be the micronutrient with the largest deficiencies worldwide. Anemia is actually a major global public health problem, affecting 20% of the world's population.[14]

Iron-deficiency anemia is caused by insufficient dietary intake and absorption of iron. To increase daily iron intake,

[a]Departamento de Química Inorgánica, Instituto de Biotecnología, Facultad de Ciencias, Universidad de Granada, 18071 Granada, Spain
[b]Department of Pharmacology, CIBER-EHD, ibs. GRANADA, CIBM, University of Granada, Spain
[c]Instituto de Nanociencia de Aragón, Universidad de Zaragoza, 50018 Zaragoza, Spain
[d]Biosearch S. A. Camino de Purchil, 66, 18004 Granada, Spain

numerous supplements based on different classical chemical iron forms are commercially available. It is well known that the limitations of these iron supplements are their low bioavailability and gastrointestinal side effects.[15] Iron oxide nanoparticles have emerged as a promising route for iron supplements since they are more bioactive than classical chemical forms and have a much greater access to tissues.

Iron absorption takes place at the small intestine, preferentially in the duodenum. It is therefore still a challenge to develop routes for overcoming the strong acidic gastric environment of the stomach and drive the iron nanoparticles to the intestines. Parallel to this development, it is necessary to gain more insights about the processes of distribution and degradation of magnetic nanoparticles along the GI. Two approaches can be envisaged to succeed in overcoming this challenge: the use of magnetic nanoparticles with protective coatings for avoiding the chemical attack at the stomach or the use of bioplatforms as carriers towards the intestines. In this regard, we have recently reported how probiotic bacteria, *Lactobacillus fermentum* or *Bifidobacterium breve*, serve as platforms to densely arrange magnetic nanoparticles on their external surfaces.[16] This is a promising route to allow the magnetic nanoparticles to pass through the stomach medium and reach the intestines, since probiotic bacteria constitute an important part of natural microbiota, which survive the stomach conditions and nest in different areas of intestines.

In this paper, we describe a magnetic study in parallel to monitor the biodistribution and biodegradation of nude 10 nm maghemite nanoparticles (MNP) and probiotic bacteria containing thousands of these same nanoparticles (MNP–bacteria), over the bowel system after oral administration in rats. The aim of this study is to compare the biodistribution and biodegradation patterns of maghemite nanoparticles when administered orally as single nanoparticles (MNP) or aggregated onto a bioplatform, such as *Lactobacillus fermentum* (MNP–bacteria).

To achieve this objective, we used AC magnetic susceptibility measurements (the in- and out-of-phase susceptibility, $\chi'(T)$ and $\chi''(T)$ respectively) of different tissues obtained after rat sacrifice. In particular, we extracted the stomach, small intestine, large intestine and cecum. The temperature dependence of the out-of-phase susceptibility ($\chi''(T)$) is a high-sensitive parameter for the detection of magnetic nanoparticles in tissues[17,18] because: (i) other paramagnetic iron species present in enterocytes do not contribute to $\chi''(T)$; (ii) the maghemite nanoparticle objects of this study are distinguished from other superparamagnetic native species present in enterocytes such as ferritin, based on their blocking temperatures, which serve as fingerprints for the identification of the presence of these nanoparticles in tissue samples; (iii) the maxima in $\chi'(T)$ and $\chi''(T)$ susceptibility curves give information on particle size and degree of aggregation and (iv) AC magnetic susceptibility of the administered nanoparticles per mass of iron, provides a calibration curve for the quantitative determination of the presence of the particles in tissue samples.

Materials and methods

MNP and MNP–bacteria preparation

MNP and MNP–bacteria were prepared following a previously described procedure.[16,18] MNP were synthesized according to Massart's method by co-precipitation of Fe(II) and Fe(III) salts in a stoichiometry of 0.5.[18] By adjusting the pH to 11 with 3 M NaOH and ionic strength with 1 M $NaNO_3$, the average size of the resulting magnetite nanoparticles is 10 nm. After oxidation of magnetite to maghemite with 1 M $HClO_4$, a colloid of maghemite nanoparticles stable at pH 2 was obtained.[20]

For the preparation of MNP–bacteria, a liquid culture of probiotic *Lactobacillus fermentum* CECT5716 was grown in a common bacterial growth medium such as MRS at 37 °C with orbital agitation for 24 h. Bacteria were centrifuged at 3000*g* for 5 min and washed with distilled water. Then, an acid solution (pH 2) of MNP (66.6 μL, 0.95 M) was added to the bacteria in an ice bath and mixed. The solution was diluted to 1 mL with distilled water. Bacteria labelled with maghemite nanoparticles (MNP–bacteria) were collected at 100*g*, 20 min.

MNP and MNP–bacteria characterization was carried out by Transmission Electron Microscopy (TEM) as previously reported.[16]

Animals

This study was carried out in accordance with the 'Guide for the Care and Use of Laboratory Animals' as promulgated by the National Institute of Health and the protocols approved by the Ethics Committee of Laboratory Animals of the University of Granada (Spain) (ref. no. CEEA-2010-286). All studies involving animals are reported in accordance with the ARRIVE guidelines for reporting experiments involving animals.[21,22]

Male Wistar rats (180–200 g) obtained from Janvier (St Berthevin Cedex, France) were housed individually in Makrolon cages, maintained in an air-conditioned atmosphere with a 12 h light–dark cycle, and provided with free access to tap water and food *ad libitum*. They were randomly assigned to different experimental groups (n = 4). One of them received only the standard diet, whereas the three remaining groups were fed an iron deficient diet (TD.80396) provided by Harlan Laboratories (Madison, WI, USA). Two rats of this group received a supplement of iron (1 mg per day per animal) by suspensions of MNP or MNP–bacteria. All samples were administered daily by oral gavage. Food and water intake was recorded daily for all groups. Rat body weight was measured twice a week. No significant differences were observed in animal weight among the groups throughout the experiment. Blood samples were taken after two weeks from the hepatic portal vein in a heparinized tube to analyze the blood picture. Then, the rats were sacrificed and the stomach, small intestines, cecum and large intestines were collected, weighed and immediately frozen in liquid nitrogen and stored at −80 °C.

Elemental analysis

Freeze-dried tissue samples together with MNP–bacteria and MNP were weighed and acid digested for elemental analysis by adding 65% HNO_3 (w/v) and heating up to 95 °C for 1 h using

a hot block. After that, the samples were allowed to cool down to room temperature and 30% H_2O_2 (w/v) was added and heated up to 95 °C for 1 h. Inductively coupled Plasma Optical Emission Spectroscopy (ICP-OES) in a Perkin Elmer Optima 2100 DV was used to determine the iron concentration.

Agar dilutions

To evaluate the influence of dipolar interactions on the particle magnetic properties dilutions in 2% w/v agar of the MNP and MNP–bacteria were prepared. MNP and MNP–bacteria were mixed with liquid agar solution (at about 90 °C). The mixture was then quickly placed in a warm ultrasonic bath that allowed the slow jellification of the agar while the materials were dispersed by the ultrasound. The resulting gels were freeze-dried for 24 h in a Telstar lyoquest lyophilizer.

Magnetic characterization

Tissue samples, MNP–bacteria and MNP were freeze-dried and the corresponding powders were placed in gelatine capsules for magnetic characterization. Measurements were performed in a Quantum Design MPMS-XL SQUID magnetometer equipped with an AC (alternating current) magnetic susceptibility option. AC susceptibility measurements were performed with an AC amplitude of 0.41 Oe, in the temperature range between 10 and 300 K and at a frequency of 11 Hz.

Dipolar interactions were checked by calculating the parameter τ_0, which is the pre-exponential factor from the Arrhenius equation for the relaxation time, $\tau = \tau_0 \exp(E_a/k_BT)$, where k_B is the Boltzmann constant and E_a the single particle anisotropy energy barrier. Calculations were performed in selected samples only when the experimental noise was low enough to perform an accurate data fit. This analysis is based on the complementarity of the relaxational information contained in the in-phase and out-of-phase magnetic susceptibility data and has been previously described.[23]

Results and discussion

TEM analysis of MNP and MNP–bacteria

TEM images of MNP mainly showed irregular spherical nanoparticles (Fig. 1). The mean particle size was 10.0 nm (σ = 0.9).

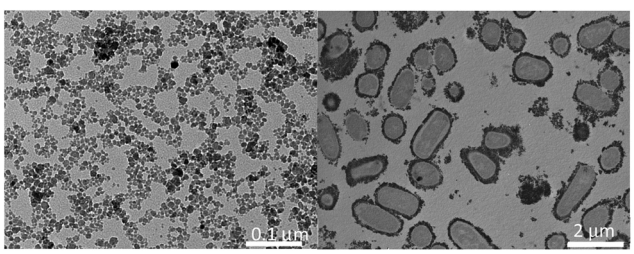

Fig. 1 A typical TEM micrograph (left) of maghemite nanoparticles (MNP). On the right, a micrograph of a thin epoxy resin section showing the presence of particles at the external surface of bacteria (MNP–bacteria).

For MNP–bacteria, large accumulations of nanoparticles were seen by TEM at the external surfaces of the bacteria (Fig. 1). Only a small fraction of nanoparticles is in the inter-bacterial region, while inside the bacteria, nanoparticles are hardy observable. The MNP adhere to the bacterial external surface, probably at the EPS, due to the electrostatic interaction between positive MNP and negative bacterial EPS.[16]

Fe analysis of tissues

Iron contents in every gastrointestinal tissue of rat controls and rats administered with MNP and MNP–bacteria were measured by ICP-OES. As shown in Fig. 2, the total amount of iron in intestines (the addition of the iron content in cecum, small and large intestines) is sensibly higher when administered with MNP–bacteria (0.620 mg Fe per g tissue) than with MNP (0.414 mg Fe per g tissue). The difference is particularly significant in the cecum, where the amount of iron after administration of MNP–bacteria (0.384 mg Fe per g tissue) is twice that obtained after administration of MNP (0.203 mg Fe per g tissue). This finding is in agreement with the known fact that probiotic bacteria preferentially nest in the different areas of the GI, and suggests that the probiotic bacteria act as a useful carrier to assist the magnetic nanoparticles in overcoming the stomach medium.

Magnetic study of tissues

The magnetic properties of MNP and MNP–bacteria were characterized by AC magnetic susceptibility. The in-phase susceptibility of both samples show a single maximum accompanied by a maximum at slightly lower temperatures for the out-of-phase component, indicative of the magnetic relaxation phenomenon of magnetic blocking of superparamagnetic particles (Fig. 3). The out-of-phase susceptibility becomes zero above 250 K, indicating that these samples are superparamagnetic above these temperatures. Slight differences are observed between the two samples regarding the temperature position of the maxima. Specifically, $\chi'(T)$ maxima were located at ~160 and ~200 K for MNP and MNP–bacteria

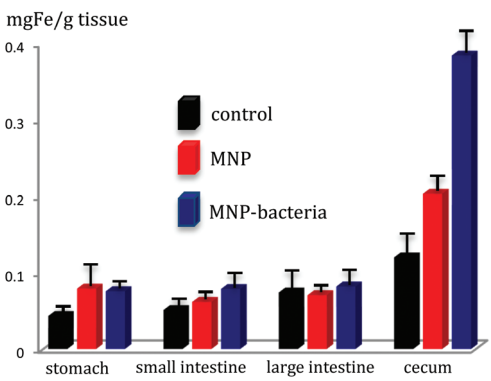

Fig. 2 Iron content in bowel tissues after MNP and MNP–bacteria administration. Black bar: rat controls; red bar: rats administered with MNP and blue bar: rats administered with MNP–bacteria. Error bars, ±sem.

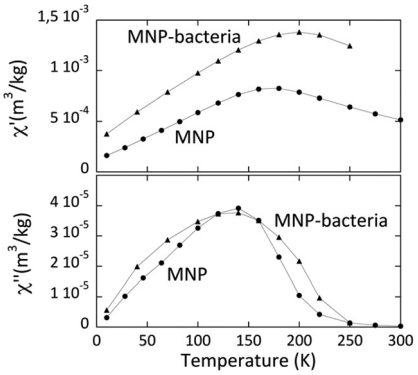

Fig. 3 Temperature dependence of the in-phase and out-of-phase magnetic susceptibility of MNP (circles) and MNP–bacteria (triangles) per mass of sample.

respectively. This behaviour is in agreement with the expected variations in the dipolar magnetic interactions among nanoparticles produced by different degrees of aggregation when comparing isolated (MNP) or grafted to the external bacterial surface (MNP–bacteria).[16,17]

Further analysis of the interparticle interactions has been performed through the characterization of the same materials diluted in agar to try to reduce the interparticle interactions (Fig. 4). It can be observed that the dilution in agar results in a shift towards lower temperatures of the $\chi''(T)$ maximum only for the MNP, but not for the MNP–bacteria. This fact is easily understood given that the agar dilution of MNP–bacteria reduces the distance between bacteria but keeps the interparticle distances unchanged, as they remain on the bacteria surface. However in the case of the MNP, the $\chi''(T)$ maximum shifts from 140 K for the concentrated sample to around 60 K for the diluted one (Fig. 4) as a consequence of the higher interparticle distances.

The importance of the interparticle interactions has also been evaluated through the determination of the pre-exponential factor, τ_0 of the Arrhenius equation. In this case, τ_0 for the original MNP and MNP–bacteria present values outside the negligible dipolar interaction range (10^{-9}–10^{-12} s) being around 10^{-24} and 10^{-21} s respectively. However, the dilution of MNP in agar served to reduce the interparticle interactions, as this sample presents a τ_0 value of 1.6×10^{-12} s, located within the negligible interaction limit.

The χ' and χ'' profiles of the different organs are close to those of administered materials, as all of them show a single in-phase and out-of-phase maxima (Fig. 5). Interestingly, two different features stand out. First, the location in temperature of the χ'' maximum from both cecum samples is located at significantly lower temperatures (below 50 K) than the rest of the tissues, with maxima located between 100 and 150 K (Table 1). The location at lower temperatures indicates a transformation of the administered particles that could be associated with a reduction of the particle size, a reduction of the interparticle interactions, or both. The second interesting feature appears in the cecum sample from the animal that received the MNP treatment, where a paramagnetic tail is observed in $\chi'(T)$ at low temperatures, indicative of the presence of non-mineral iron species.

It is also worth mentioning that the height of the out-of-phase susceptibility maxima may be used as a surrogate of the iron concentration in the form of a given species.[23] In this study, in animals from both treatments, both the large and small intestines present a similar concentration of iron magnetic nanoparticles while the stomach seems to be the organ

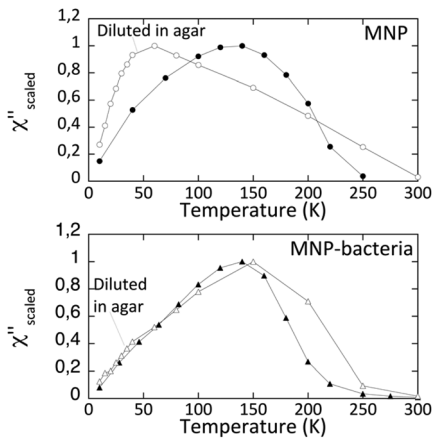

Fig. 4 Temperature dependence of the out-of-phase magnetic susceptibility of MNP and MNP–bacteria (black) and their corresponding dilutions in agar (white) scaled to their maximum.

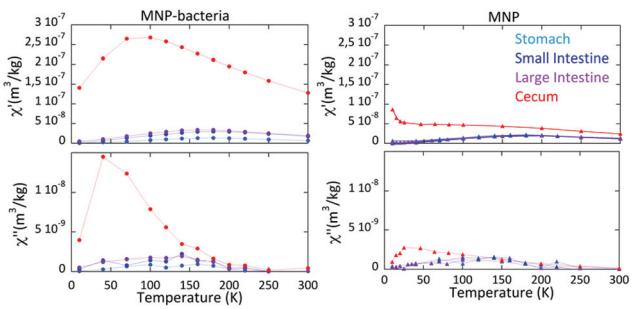

Fig. 5 Temperature dependence of the in-phase and out-of-phase magnetic susceptibility per mass of tissue for different organs from the rats treated with MNP (right) and MNP–bacteria (left).

Table 1 Temperature maxima of $\chi'(T)$ and $\chi''(T)$ curves after MNP or MNP–bacterial treatment for different tissues

	Temperature (K) of χ' and χ'' maxima			
	MNP		MNP–bacteria	
Tissue	χ'	χ''	χ'	χ''
Stomach	180	≈140	180	≈140
Small intestine	180	≈140	180	≈140
Large intestine	180	≈130	160–180	≈140
Cecum	50–100	30–50	70–100	<50

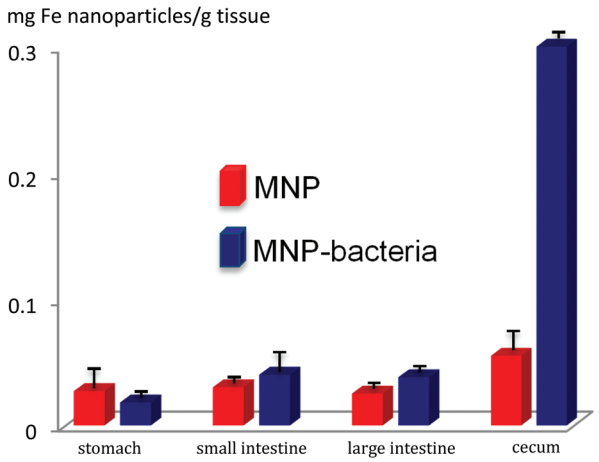

Fig. 6 Iron concentration, in the form of magnetic nanoparticles, in every tissue, calculated from the magnetic measurements. Error bars, ±sem.

with a smaller amount of particles and the cecum the organ that accumulates the biggest amount.

Using the magnetic susceptibility data we can quantify the iron concentration in the form of nanoparticles in every tissue following the protocols described elsewhere (Fig. 6).[17,24] This quantitative determination of iron can be performed given the existence of standards, in this case MNP and MNP–bacteria, with the same magnetic behaviour as observed in most of the tissue samples. Although we can quantify with a relatively low error the iron content in the stomach, small and large intestines, this is not possible in the cecum, due to the different temperature locations of the maximum observed in this tissue when compared with the administered materials. For this organ, the determination of mg of Fe nanoparticles per g of dry tissue is therefore not as rigorous as for the other tissues.

The first conclusion drawn from these data is that the amount of magnetic nanoparticles in intestine tissues (small, large and cecum) is higher after administration of MNP–bacteria than MNP. As in the iron content analysis by ICP-OES, the difference is particularly significant in the cecum, where the values of the out-of-phase magnetic susceptibility are five times higher. The only tissue where nanoparticle accumulation is higher when administrating MNP than MNP–bacteria is precisely the stomach, 0.027 against 0.018 mg g^{-1} stomach for MNP and MNP–bacteria respectively, which is another piece of evidence that bacteria act as a useful carrier to assist the magnetic nanoparticles in overcoming the stomach medium and reaching the intestines.

From a qualitative point of view, the pattern of biodistribution of maghemite nanoparticles after ingestion of MNP and MNP–bacteria seems similar at first sight: nanoparticles distribute along the GI and specifically accumulate in the cecum. However, in a deeper analysis, some drastic differences are noted. First, the accumulation of magnetic nanoparticles in the cecum is more specific when MNP–bacteria were administered, since the values of $\chi''(T)$ for the cecum is ten times larger than for other tissues, whereas this difference is only double when MNP were administered. Second, the maxima of $\chi''(T)$ in the cecum (around 50 and 30 K after administration of MNP–bacteria and MNP, respectively) are located at lower temperatures with respect to the original MNP or MNP-bacteria samples (200 and 160 K, respectively), and are also below the MNP sample diluted in agar, which presents negligible interactions. This fact points out the existence of a degradation process of magnetic nanoparticles. The fact that the out-of phase susceptibility maxima is below the non-interaction limit determined by the τ_0 value for the MNP agar dilution, indicates that in addition to a disaggregation process of the MNP and maybe a release of particles from the MNP–bacteria, a reduction of the particle size as a consequence of the biodegradation process also occurs. The reduction of the particle size would result in a release of free iron atoms, a fact that agrees with the paramagnetic tail observed in $\chi'(T)$ at low temperatures in the cecum sample from the animals that received the MNP treatment and that has been previously observed in MNP samples degraded artificially.[18] In contrast, the absence of a paramagnetic tail in the cecum $\chi'(T)$ curve after MNP–bacteria administration points to the existence of a higher accumulation of less-degraded magnetic nanoparticles.

These same conclusions can also be drawn from comparing the ratios between iron concentrations from maghemite nanoparticles (estimated by SQUID measurements) and total iron (measured by ICP-OES), in every tissue, after MNP or MNP–bacteria administration (Table 2). This ratio is bigger at the stomach for MNP, meaning that maghemite nanoparticles accumulate more in this organ when administered with MNP than with MNP–bacteria. In contrast, the intestines present bigger ratios for the MNP–bacteria treatment, this difference being significantly higher for the cecum, where the MNP may have degraded faster or accumulated in a lower amount than the MNP–bacteria.

Table 2 Comparison of total iron contents (mg Fe per g sample) in bowel tissues (measured by ICP-OES) and iron as maghemite nanoparticles (obtained from SQUID measurements)

Tissue	Treatment	[Fe] maghemite	[Fe] total	[Fe] maghemite/[Fe] total
Stomach	Control	0.00	0.05	0.00
	MNP	0.03	0.09	0.33
	MNP–bact	0.02	0.08	0.25
Small intestine	Control	0.00	0.06	0.00
	MNP	0.03	0.07	0.43
	MNP–bact	0.04	0.08	0.50
Large intestine	Control	0.00	0.07	0.00
	MNP	0.03	0.06	0.50
	MNP–bact	0.04	0.07	0.60
Cecum	Control	0.00	0.13	0.00
	MNP	0.06	0.20	0.30
	MNP–bact	0.30	0.40	0.75

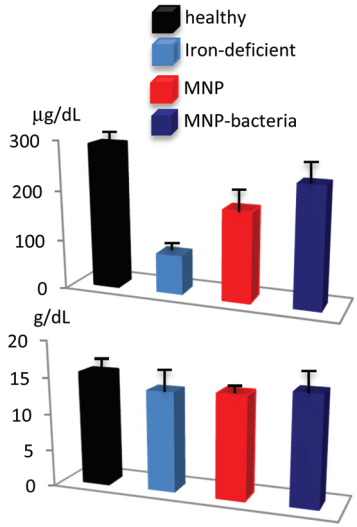

Fig. 7 Iron plasma (top) and haemoglobin (bottom) values measured in rats: healthy, iron-deficient and treated with MNP and MPN-bacteria. Error bars, ±sem.

In view of these findings and taking into account that nanoparticles passes through the GI tract following the order: stomach, small intestine, cecum and finally large intestine, it is an interestingfact that the maxima in the $\chi'(T)$ and $\chi''(T)$ curves are located at lower temperatures in the cecum than in the following tissue (large intestine). It could be postulated that a small fraction of the MNP and MNP bacteria pass through the whole GI and is probably excreted through the feces, while most of it, especially MNP–bacteria, overcome the stomach medium and accumulate in the cecum.

Since iron absorption takes place in the small intestine, especially the duodenum, iron supplements must pass through the stomach and reach the small intestine. Our findings show that the concentration of maghemite nanoparticles at the small intestine is higher when administered with MNP–bacteria than with MNP. Accordingly this MNP–bacteria should be more effective for iron supply than MNP. To confirm this, iron plasma and haemoglobin levels were measured in four groups of rats: healthy, iron-deficient and iron-deficient rats after administration of MNP or MNP–bacteria. Results presented in Fig. 7 show improvement in iron status after treatment with MNP–bacteria. In fact, both iron plasma and haemoglobin levels were corrected to healthy values in rats fed MNP–bacteria over two weeks, while those under treatment with MNP failed to reach normal values after the same period.

Conclusions

The collective analysis of iron contents and magnetic susceptibilities of the different GI tissues (stomach, small and large intestines and cecum) reveals different biodistribution and biodegradation patterns of the maghemite nanoparticles after their ingestion as simple MNP or as MNP–bacteria entities. The results confirm that the use of probiotic bacteria is a suitable strategy to assist the magnetic nanoparticles to overcome the stomach medium for achieving their accumulation in intestines, especially in the cecum. We believe that these findings have a wide applicability in biodistribution and biodegradation studies involving oral magnetic nanostructures and establish a framework for their applications in medicine. As an example of this, we have illustrated how the administration of MNP–bacteria to iron-deficient rats corrects the iron levels after two weeks of treatment.

Acknowledgements

This work was funded by Biosearch S.A. (CARMENTA Project – FEDER INTERCONECTA), MINECO and FEDER (project CTQ2015-64538-R) and Junta de Andalucía (AGR-6826 and CTS 164). The CIBEREHD is funded by the Instituto de Salud Carlos III. Lucía Gutiérrez acknowledges financial support from the Ramon y Cajal subprogram (RYC-2014-15512).

Notes and references

1 S. Laurent, L. Vander Elst and R. N. Muller, in *Chemistry of Contrast Agents in Medical Magnetic Resonance Imaging*, ed. A. Merbach, L. Helm and E. Toth, 2nd edn, 2013, pp. 427–447.
2 F. Liu, S. Laurent, H. Fattahi, L. Vander Elst and R. N. Muller, *Nanomedicine*, 2011, **6**, 519–528.
3 S. Laurent, J.-L. Bridot, L. Vander Elst and R. N. Muller, *Future Med. Chem.*, 2010, **2**, 427–449.
4 S. Laurent, D. Forge, M. Port, A. Roch, C. Robic, L. Vander Elst and R. N. Muller, *Chem. Rev.*, 2009, **110**, 2574.
5 S. J. J. Titinchi, M. P. Singh, H. S. Abbo and I. R. Green, *Adv. Healthcare Mater.*, 2014, **3**, 49–85.
6 F. Canfarotta and S. A. Piletsky, *Adv. Healthcare Mater.*, 2014, **3**, 160–175.
7 M. Colombo, S. Carregal-Romero, M. F. Casula, L. Gutiérrez, M. P. Morales, I. B. Bönhm, J. T. Heverhagen, D. Prosperi and W. J. Parak, *Chem. Soc. Rev.*, 2012, **41**, 4306–4334.
8 Q. Pankhurst, N. Thanh, S. Jones and J. Dobson, *J. Phys. D: Appl. Phys.*, 2009, **42**, 224001.
9 J. Kolosnjaj-Tabi, L. Lartigue, Y. Javed, N. Luciani, T. Pellegrino, C. Wilhelm, D. Alloyeau and F. Gazeau, *Nano Today*, 2015, DOI: 10.1016/j.nantod.2015.10.001. Q5
10 S. Chamorro, L. Gutiérrez, M. P. Vaquero, D. Verdoy, G. Salas, Y. Luengo, A. Brenes and F. J. Teran, *Nanotechnology*, 2015, **26**, 205101.
11 P. Guardia, A. Riedinger, H. Kakwere, F. Gazeau and T. Pellegrino, in *Bio- and Bioinspired Nanomaterials*, ed. D. Ruiz-Molina, F. Novio and C. Roscini, 2015, pp. 139–172.
12 X. Liu, I. Marangon, G. Melinte, C. Wilhelm, C. Menard-Moyon, B. P. Pichon, O. Ersen, K. Aubertin, W. Baaziz,

C. Pham-Huu, S. Begin-Colin, A. Bianco, F. Gazeau and D. Begin, *ACS Nano*, 2014, **8**, 11290–11304.
13 World Cancer Report 2014, World Health Organization, 2014. pp. chapter 1.1.
14 E. McLean, M. Cogswell, I. Egli, D. Wojdyla and B. De Benoist, WHO Vitamin and Mineral Nutrition Information System, 1993–2005, *Public Health Nutr.*, 2009, **12**, 444–454.
15 R. Hoffman, E. Benz and S. Shattil, *et al.*, *Disorders of iron metabolism: iron deficiency and overload*, in *Hematology*, Churchill Livingstone, Philadelphia-USA, Harcourt Brace & Co, New York, NY, USA, 3rd edn, 2000, ch. 26.
16 M. Martín, F. Carmona, R. Cuesta, D. Rondón, N. Gálvez and J. M. Dominguez-Vera, *Adv. Funct. Mater.*, 2014, **24**, 3489.
17 L. Gutiérrez, M. P. Morales and F. J. Lázaro, *Phys. Chem. Chem. Phys.*, 2014, **16**, 4456.
18 L. Gutiérrez, S. Romero, G. B. da Silva, R. Costo, M. D. Vargas, C. M. Ronconi, C. J. Serna, S. Veintemillas-Verdaguer and M. P. Morales, *Biomed. Tech.*, 2015, **60**, 417–425.
19 F. Carmona, M. Martin, N. Galvez and J. M. Dominguez-Vera, *Inorg. Chem.*, 2014, **53**, 8565.
20 R. Massart, *IEEE Trans. Magn.*, 1981, 1247–1248.
21 L. Vayssieres, C. Chaneac, E. Tronc and J. P. Jolivet, *J. Colloid Interface Sci.*, 1998, **205**, 205–212.
22 C. Kilkenny, W. J. Browne, I. C. Cuthill, M. Emerson and D. G. Altman, *J. Pharmacol. Pharmacother.*, 2010, **1**, 94.
23 J. C. McGrath, G. B. Drummond, E. M. McLachlan, C. Kilkenny and C. L. Wainwright, *Br. J. Pharmacol.*, 2010, **160**, 1573.
24 A. López, L. Gutiérrez and F. J. Lázaro, *Phys. Med. Biol.*, 2007, **52**, 5043–5056.